*Annals of Botany* **119**: 841–852, 2017
doi:10.1093/aob/mcw202, available online at www.aob.oxfordjournals.org

ANNALS OF BOTANY
Founded 1887

PART OF A SPECIAL ISSUE ON PLANT IMMUNITY

# Infection by *Rhodococcus fascians* maintains cotyledons as a sink tissue for the pathogen

**Pragatheswari Dhandapani[1], Jiancheng Song[1,2], Ondrej Novak[3] and Paula E. Jameson[1,*]**

*[1]School of Biological Sciences, University of Canterbury, Private Bag 4800, Christchurch 8140, New Zealand, [2]School of Life Sciences, Yantai University, Yantai 264005, China and [3]Laboratory of Growth Regulators, Centre of the Region Haná for Biotechnological and Agricultural Research, Institute of Experimental Botany CAS & Faculty of Science of Palacký University, Šlechtitelů 27, 783 71 Olomouc, Czech Republic*
**For correspondence. E-mail paula.jameson@canterbury.ac.nz*

Received: 7 April 2016 Returned for revision: 31 July 2016 Accepted: 5 August 2016 Published electronically: 16 November 2016

• **Background and Aims** *Pisum sativum* L. (pea) seed is a source of carbohydrate and protein for the developing plant. By studying pea seeds inoculated by the cytokinin-producing bacterium, *Rhodococcus fascians*, we sought to determine the impact of both an epiphytic (avirulent) strain and a pathogenic strain on source–sink activity within the cotyledons during and following germination.
• **Methods** Bacterial spread was monitored microscopically, and real-time reverse transcription–quantitative PCR was used to determine the expression of cytokinin biosynthesis, degradation and response regulator gene family members, along with expression of family members of *SWEET*, *SUT*, *CWINV* and *AAP* genes – gene families identified initially in pea by transcriptomic analysis. The endogenous cytokinin content was also determined.
• **Key Results** The cotyledons infected by the virulent strain remained intact and turned green, while multiple shoots were formed and root growth was reduced. The epiphytic strain had no such marked impact. Isopentenyl adenine was elevated in the cotyledons infected by the virulent strain. Strong expression of *RfIPT*, *RfLOG* and *RfCKX* was detected in the cotyledons infected by the virulent strain throughout the experiment, with elevated expression also observed for *PsSWEET*, *PsSUT* and *PsINV* gene family members. The epiphytic strain had some impact on the expression of these genes, especially at the later stages of reserve mobilization from the cotyledons.
• **Conclusions** The pathogenic strain retained the cotyledons as a sink tissue for the pathogen rather than the cotyledon converting completely to a source tissue for the germinating plant. We suggest that the interaction of cytokinins, CWINVs and SWEETs may lead to the loss of apical dominance and the appearance of multiple shoots.

**Key words:** Apical dominance, amino acid transporter, cell wall invertase, cytokinin, cytokinin oxidase/dehydrogenase, *Pisum sativum* L., pea, *Rhodococcus fascians*, seed, sink and source, SWEET, sucrose transporter.

## INTRODUCTION

Changes in source–sink dynamics are an integral component of the plant life cycle. During its developmental phase, the seed of an annual plant is the major sink for assimilates. In contrast, during germination, the seed changes to function as a source for the developing seedling. However, impacting on the developmental control of source–sink relationships exercised by the plant is the challenge invoked by plant pathogens. Here, cellular, biochemical and physiological changes may occur within the plant, as the pathogen competes with the plant for assimilates.

For many years, the cytokinins have been functionally implicated in source–sink dynamics during plant development (Mothes and Engelbrecht, 1963; Ehness *et al*., 1997; Balibrea Lara *et al*., 2004; Werner and Schmülling, 2009; Jameson and Song, 2016), as well as being implicated in plant–pathogen (bacteria, fungal and viral) interactions and particularly in the establishment of a suitable niche for gall-forming pathogens (Jameson, 2000). In plants, cytokinins are biosynthesized directly by isopentenyl transferase (IPT) attaching an isoprenoid side chain to the N6 position of an adenine nucleotide moiety. The cytokinin side chain may become hydroxylated or unsaturated. The cytokinin nucleotides may be activated to the free base forms by LONELY GUY (LOG), or to the riboside forms. The cytokinin molecule may be inactivated by the removal of the side chain by cytokinin oxidase/dehydrogenase (CKX), or metabolized to storage *O*-glucosides (which can be released to active forms by β-glucosidases) or 7- and 9-glucosides (which appear not to be reactivated). The free bases are considered the active forms perceived by cytokinin receptors (Lomin *et al*., 2015) and the ribosides the translocated forms. Cytokinins may also be formed by tRNA-IPTs. Cytokinins released from tRNA may supplement the endogenous cytokinin pool. For recent overviews, see Spichal (2012) and Jameson (2017).

Germinating seeds are metabolically highly active, degrading carbohydrate, lipid and proteins stores and mobilizing these to the embryo and from there to the emerging root and shoot (Weitbrecht *et al*., 2011). Pea seeds, which store starch and protein, exhibit increased respiration and metabolic activity within hours of imbibition (Nawa and Asahi, 1971), followed by reserve mobilization as roots and shoots emerge (Weitbrecht

*et al*., 2011). The embryo axis of germinating lupin seeds is capable of biosynthesizing cytokinin (Nandi *et al*., 1988; Nandi and Palni, 1989). The cytokinins, which were transported to the cotyledons, were shown to be highly stable and to induce cotyledon expansion and chlorophyll synthesis (Nandi and Palni, 1989).

As our earlier work had noted that the cotyledons of pea (*Pisum sativum* L.) infected with a virulent strain of *Rhodococcus fascians* became green and retained their integrity (Eason *et al*., 1995), we hypothesized that cytokinins emanating from the bacterium induced the chlorophyll synthesis, and that the bacterium also caused the germinating pea to change from being a source of metabolites for the developing root and shoot to becoming a sink of metabolites for the pathogen. *Rhodococcus fascians* is a Gram-positive, non-host-specific, bacterium that can exist as both epiphytic and endophytic colonies. To determine the impact of *R. fascians* inoculation of germinating pea seeds on cytokinin biosynthesis and metabolism, we analysed the expression of *PsIPT*, *PsCKX* and *PsLOG* gene family members in *P. sativum* simultaneously with the expression of the *R. fascians fas* genes [*RfIPT* (*FasD*), *RfLOG* (*FasF*) and *RfCKX* (*FasE*); Pertry *et al*., 2010; Stes *et al*., 2011] using the primers designed specifically to discriminate between the plant and microbial cytokinin genes. The expression of *P. sativum* response regulator (*PsRR*) genes was also monitored to assess if the cytokinin signal transduction pathway was affected by *R. fascians*, and the endogenous cytokinins identified and quantified.

A transcriptome analysis conducted by Depuydt *et al*. (2009) showed both upregulated and downregulated genes following infection of arabidopsis by virulent strain D188 of *R. fascians*, including upregulation of genes coding for sugar transporter proteins, but downregulation of amino acid transporter family proteins. Importantly, Depuydt *et al*. (2009) also showed that the avirulent strain D188-5 had an impact on primary metabolism and, recently, Francis *et al*. (2016) suggested that D188-5 has a plant growth-promoting effect. To assess the impact of *R. fascians* on the source–sink dynamics of the germinating pea, expression of sucrose and amino acid transporter gene family members (*SUT* and *AAP*), cell wall invertase (*CWINV*) and *SWEET* were monitored. Enhanced expression of *CWINV* has been reported in several plant–pathogen interactions (Berger *et al*., 2007; Depuydt *et al*., 2009; Chandran *et al*., 2010; Siemens *et al*., 2011). Interaction between cytokinins and CWINV is well documented, in relation to both cell division (Roitsch and González, 2004; Jameson and Song, 2016) and source–sink dynamics (Ehneß and Roitsch, 1997; Albacete *et al*., 2015). Cytokinins failed to delay senescence when CWINV was inhibited (Balibrea Lara *et al*., 2004), indicating that nutrient mobilization is essential in cytokinin-induced senescence delay, providing the basis for pathogen-induced 'Green Island' formation (Roitsch and González, 2004), and potentially the greening of the infected pea cotyledons.

We also chose to monitor the *SWEET* (Sugar Will Eventually be Exported Transporter) gene family as it was recently identified as a sugar efflux protein (Chen *et al*., 2010) and pathogens have been shown to modulate sugar efflux in the host plant to promote their own growth (Chandran, 2015; Eom *et al*., 2015). The *SWEET* family members cluster into four clades (Eom *et al*., 2015). Different *SWEET* gene family members transport hexoses (Chen *et al*., 2010) and sucrose (Chen *et al*., 2012). Clade II members are hexose transporters and Clade III transport sucrose, in both cases across the plasma membrane to the apoplasm, whereas members of Clade IV transport hexoses across the tonoplast into the vacuole (Guo *et al*., 2014). Clade I members transport hexoses and are localized either to the plasma membrane (Chen *et al*., 2010) or to the tonoplast (Chen *et al*., 2015). When SWEET function is blocked, growth and virulence of some pathogens have been shown to be reduced. For example, work with bacterial blight of rice caused by *Xanthomonas oryzae* pv. *oryzae* indicates that this pathogen enhances the release of sucrose from the host cells by inducing expression of *OsSWEET13*, a member of Clade III. Targeted mutation of *OsSWEET13* led to reduced pathogenesis (Zhou *et al*., 2015). Earlier it was shown that two other Clade III SWEETs (OsSWEET11 and OsSWEET14) were also targets of bacterial rice blight (Li *et al*., 2013; Streubel *et al*., 2013).

Chandran (2015) suggested that co-option of SWEETs may be a 'universal strategy adopted by diverse types of pathogens' and that different pathogens have co-opted different *SWEET* gene family members to provide carbohydrate. However, in contrast to this, recently Chen *et al*. (2015) showed that mutants of *AtSWEET2* were more susceptible to *Pythium* infection. They suggested that expression in the roots of the Clade I member, *AtSWEET2*, restricted the amount of glucose in the apoplast, and by extension the rhizosphere, by sequestering it to the vacuole. Upon infection by *Pythium irregulare*, expression of *AtSWEET2* and *AtSWEET10* increased. *AtSWEET2* accumulated in the region of the tonoplast of the root cells where the *Pythium* was concentrated, a mechanism upregulated, the authors suggest, to sequester glucose away from the pathogen and into the vacuole. Additionally, an interaction between sucrose-transporting SWEETs and CWINV has also been invoked for pathogens that take up hexoses preferentially (Chandran, 2015).

In addition to carbon, microbes require a source of nitrogen (Fagard *et al*., 2014). Pratelli and Pilot (2014) suggested that pathogen infection leads to changes in expression of genes involved in amino acid metabolism and transport. They also tabulated the effect of nematode infection on *AtAAP* gene family members, showing that these responded differentially (induced or repressed) by infection. As functional studies have shown that AtAAPs can transport a wide range of amino acids (Tegeder, 2012; Tegeder and Ward, 2012), we were interested in whether these transporters were activated following inoculation by *R. fascians*.

It has been noted that cytokinin-mediated resistance in arabidopsis and tobacco operates differently (Großkinsky *et al*., 2011), and consequently may also differ in legumes. We chose to work with pea as it has historically been the test organism for *R. fascians* infection (Lacey, 1936). As *R. fascians* is a soil-borne microbe, we inoculated pea seeds at the time of imbibition with *R. fascians* avirulent strain 589 and virulent strain 602. Strain 602 is highly virulent (Eason *et al*., 1996; Stange *et al*., 1996), and has a 210 kb linear plasmid containing *RfIPT*, *RfLOG* and *RfCKX*, whereas avirulent strain 589 lacks a linear plasmid and all three genes (Galis *et al*., 2005; Stange *et al*., 1996; Supplementary Data Table S1). Both strains extrude multiple cytokinin types into the culture medium, with the production of non-hydroxylated [isopentenyl adenine (iP)-type] cytokinins about 1000 times greater than that of hydroxylated

[zeatin (Z)-type] cytokinins (Eason *et al*., 1996). Along with a microscopic investigation, gene expression and endogenous cytokinins were monitored in the imbibed and germinating seeds inoculated by the *R. fascians* strains and mock-inoculated controls.

## MATERIALS AND METHODS

### *Plant material and* Rhodococcus fascians *strains*

*Pisum sativum* variety Bohatyr was used as the host plant. Whole, surface-sterilized seeds were added to mid-log phase cultures of virulent (602) and avirulent (589) strains of *R. fascians* growing in '523' broth (Kado and Heskett, 1970) and incubated at 26 °C with shaking at 121 rpm for 4 h, a time frame coinciding with phase I water uptake during imbibition (Green and Baisted, 1972). Five to six inoculated seeds, and mock-inoculated controls, were then placed in sterilized 500 mL containers with 0·6 % (w/v) agar and 10 % (w/v) Hoagland's mineral salts solution (Lawson *et al*., 1982). The containers were placed in a growth room in a randomized block design, with three treatments (control, avirulent and virulent) and ten sampling times [4 hours post-inoculation (hpi), and 2, 5, 9, 11, 15, 20, 25, 30, 35 and 40 days post-inoculation (dpi)], each with five replications. The plants were grown at 22 °C with a 16 h photoperiod. Within 24 h, the radicle had emerged and by 2 dpi germination was complete: radicles and small plumules had both emerged from the seeds. Samples of whole plants or separated cotyledons, roots and shoots were taken for a variety of purposes, but at 2 dpi the entire germinating seed was extracted. The samples were either flash frozen in liquid nitrogen and stored at −80 °C for gene expression studies, fixed in FAA (10 % formaldehyde:5 % acetic acid:50 % alcohol) for light microscopy or cryopreserved for scanning electron microscopy (SEM). For each sampling, five plants were collected from each treatment (control, avirulent and virulent). The experiment was repeated twice, with the same procedures and sampling.

### *Light microscopy*

A modified procedure of Carletom and Druvy (1957) for fixation, dehydration, embedding and microtoming was followed. Serial sections of the embedded tissue blocks were cut to a thickness of 10–13 µm on a Lecia RM2165 microtome. After de-waxing and hydration, the sections were stained with Mayer's Haemalum (double strength) for 5 min. Sections were counter-stained with 0·5 % (v/v) Eosin Y (Sigma) in 100 % ethanol. Sections were then treated with 1:1 xylene:absolute ethanol, followed by 100 % xylene at room temperature for 3 min, mounted in Eukitt and dried in a 37 °C oven for a minimum of 2 d (Kitin *et al*., 2005). The stained sections were viewed using a Zeiss Axio Imager M1 compound microscope with brightfield (BF) and differential interference contrast (DIC) optics/lighting capabilities. Micrographs were captured using a Zeiss AxioCam HRc cooled CCD camera at 3900 × 3090 pixel resolution to facilitate later digital enlargement of specific areas to allow visualization of the fine details of *R. fascians*.

### *RNA isolation and cDNA synthesis*

RNA was extracted from pea tissues using TRIzol Reagent (Invitrogen, Carlsbad, CA, USA) following the manufacturer's instructions. The integrity and quality of isolated RNA were assessed by electrophoresis on a 1 % (w/v) agarose gel. The concentration and purity of RNA were assessed using a Nano Drop™ Spectrophotometer. The RNA was stored in 1× RNA secure™ in a –20 °C freezer. The extracted RNA was converted to cDNA by reverse transcription, using approx. 1 µg of total RNA, 50 U of Expand Reverse Transcriptase (Roche, Mannheim Germany), 50 pmol of oligo(dT) primers, and 100 pmol of random hexamer (pdN6) primers in a 20 µL reaction. The cDNA was diluted 5-fold with TE buffer and stored at –20 °C. The cDNA quality was assessed by real-time reverse transcription–quantitative PCR (RT–qPCR), where two reference genes and a target gene were used to assess the amplification curve and melting point curve of each cDNA sample.

RNA was isolated from cultures of *R. fascians* strains. Mid-log phase cultures were inoculated into '523' broth and incubated at 26 °C with shaking at 150 rpm for 4 h. The broth cultures were centrifuged at 4 °C, 15 000 rpm for 15 min. The pellets were suspended in TRIzol reagent. The procedure for plant RNA and cDNA synthesis was then followed as described above. Ribosome RNA 18S was used as the reference gene.

### *Gene isolation and sequence analysis*

Sequences of family members of candidate genes of interest were identified from RNA sequencing (RNA-Seq) transcriptomic data. An RNA pool of combined RNA samples, each extracted separately from pea cotyledons, shoots, roots, flowers and pods, and seeds at various developmental stages, was used to construct the cDNA library, which was then sequenced using an Illumina HiSeq2000 genome analyser at the Beijing Genome Institute (BGI) Customer Service.

The RNA-Seq generated a transcriptome of 4·69 Gb clean data and >52 181 000 cleaned pair-end reads, which were assembled into 95 199 contigs. In total, nearly 42 300 unigene sequences were obtained, with a median length of 777 bp. This suggests that the transcriptome data represented adequate sequencing depth and genome coverage to meet the requirement of identifying candidate gene sequences expressed in the tissue samples in the current study.

For the identification of *IPT*, *LOG*, *CKX*, *RR*, *SUT*, *INV*, *SWEET* and *AAP* gene sequences in pea, all annotated family members of these multigene families from *Arabidopsis thaliana* and the available legume orthologues from *Glycine max*, *Medicago truncatula*, *Lotus japonicus* and *P. sativum* were used as query sequences to BLAST search the transcriptome data. The putative sequences were verified to gene family level by BLAST searching the GenBank database (http://blast.ncbi.nlm.nih.gov) and multiple sequence alignment with representative orthologue sequences.

In the case of *R. fascians*, the virulent strain (602) was used as the template and primers were designed from the NCBI database to identify *IPT, LOG* and *CKX* genes, with other microbial gene orthologues being selected and used for alignment. For phylogenetic analysis, orthologues from arabidopsis, legumes, maize, rice and *R. fascians* of each gene of interest were used

to construct a Maximum Parsimony tree with either 1000 bootstrap replicates (ClustalX; Thompson *et al*., 1997) or 10 000 bootstrap replicates with MEGA4 (Tamura *et al*., 2007). Each tree was rooted with an outgroup orthologue.

### *Polymerase chain reaction*

The PCR primers specific to each family member of the genes of interest were designed using Primer Premier 5.0 based on the sequence information obtained from the transcriptome. PCRs were performed in a 20 µL mix containing 1 µL of 25 mM $MgCl_2$, 1 µL of 10 pmol $\mu L^{-1}$ of each forward and reverse primer, 2 µL of 10-fold diluted cDNA, 2 µL of 10× Taq buffer and 0·2 µL of 5 U $\mu L^{-1}$ Taq polymerase (Roche), using a PCR program consisting of 35 cycles of 94 °C for 40 s, 50–60 °C for 40 s, 72 °C for 40 s followed by one cycle of 72 °C for 5 min, then held at 4 °C. Thermocycling was performed on either a BIOrad DNA Engine Peltier Thermal Cycler or an MJ Research PTC-200 Peltier Thermal Cycler. The PCR products were separated on a 1 % (w/v) agarose gel and all the bands of approximately the expected size were purified with an UltraClean™ 15 DNA Purification Kit and sequenced at MACROGEN Inc., Korea.

### *Real-time reverse transcription–quantitative PCR*

The expression studies were conducted following the RT–qPCR MIQE guidelines (Bustin *et al*., 2009), with three technical replicates for each of two biological replicates. Primers designed for RT–qPCR were based on the PCR product sequences, and were unique and specific for the gene of interest. Primers were designed using Primer Premier 6.00 to obtain a PCR product length of around 200 bp. Primer sequences are listed in Supplementary Data Table S2. The PCR products were sequenced by MACROGEN Inc. Korea. For each gene of interest, raw sequences of at least two forward and two reverse directions were used to correct sequencing errors (Song *et al*., 2012). Sequence verification after sequencing was done for each specific target gene with BLAST (http://www.ncbi.nlm.gov/BLAST) searching the GenBank database, and each confirmed target gene was selected and designated to gene family level based on available annotated sequence or putative sequence of the target genes. The nucleotide sequences reported herein are included in Table S2.

The primers for RT–qPCR were optimized by determining the optimal annealing temperature of all the target primers and reference genes. A duplicate, no-template control was included in every run to test for DNA contamination and to assess for primer-dimers. Relative gene expression was obtained using Rotor-Gene Q (Qiagen) using either a home-made SYBR Green master mix or the KAPA SYBR® FAST qPCR Kits (Kapa Biosystems, Boston, MA, USA). A reaction volume of 10 µL was used, consisting of 5 µL of Kapa qPCR buffer (Kapa Biosystems), 2 µL of millipore water, 1 µL of cDNA and 1 µL of each forward and reverse primer. The thermal cycle consisted of an initial hold at 95 °C for 10 min, followed by 40 cycles of 95 °C for 10 s, 58 °C for 15 s and 72 °C for 20 s; then 90 s of pre-melt conditioning at 72 °C followed by melt of 72 °C to 95 °C, raising the temperature by 1 °C every 5 s.

Reference genes were used as internal controls to normalize the data by correcting for differences in quantity of cDNA used as template (Vandesompele *et al*., 2002; Gutierrez *et al*., 2008). To achieve accurate normalization, four reference genes, *Ps18S*, *PsEF*, *PsGAP* and *PsACT*, were used. The reference genes were first compared for their expression stability over different cDNA samples from tissues at different growth stages, with three replicates. The geometric mean of four reference genes was calculated according to the method described by Song *et al*. (2012), and its correlation to the target gene was compared with every gene of interest.

Relative gene expression was calculated based on the method of Pfaffl and Hageleit (2001) and Song *et al*. (2012). Gene expression was determined by comparing the expression of the gene of interest/target gene with the average expression of the four reference genes. Due to the fact that all samples could not be run in a single PCR run, an inter-run calibrator was used (Derveaux *et al*., 2010) which was composed of mixed cDNA from all tissues used in the project. The data analysis was done as described by Song *et al*. (2012). For each reference gene, a correction factor (CF) for each of the cDNA samples was calculated using the Ct value of this cDNA sample divided by the average Ct value of all cDNA samples of the same experiment. The values of three technical replicates were averaged to form the CF for each biological replicate of each reference gene. The final CF value for each biological replicate was created by averaging the CF value of four reference genes. For each cDNA sample, the Ct value of each target gene was corrected before analysis of its expression level. The expression data are presented as heat maps, with fold differences calculated relative to the mock-inoculated control.

### *Cytokinin analyses*

Cotyledons from four individual plants were ground under liquid nitrogen and freeze-dried. The four biological replicates were extracted and purified using the method published previously by Dobrev and Kamínek (2002) with some minor modifications (Antoniadi *et al*., 2015). Samples of 3–5·5 mg d. wt were extracted in 1 mL of modified Bieleski buffer (60 % MeOH, 10 % HCOOH and 30 % $H_2O$) together with a cocktail of 18 stable isotope-labelled cytokinin internal standards (0·2 pmol of cytokinin bases, ribosides, *N*-glucosides, 0·5 pmol of *O*-glucosides and nucleotides) to check recovery during purification and to validate the determination. The samples were purified using a combination of $C_{18}$ (100 mg $mL^{-1}$) and MCX cartridges (30 mg $mL^{-1}$). The eluates were evaporated to dryness and dissolved in 20 µL of the mobile phase used for quantitative analysis. The samples were analysed by the liquid chromatography–tandem mass spectrometry (LC-MS/MS system) consisting of an ACQUITY UPLC® System (Waters, MA, USA) and Xevo® TQ-S (Waters) triple quadrupole mass spectrometer. Quantification was obtained using a multiple reaction monitoring (MRM) mode of selected precursor ions and the appropriate production (Svačinová *et al*., 2012).

*Chlorophyll estimation*

The chlorophyll content of cotyledon samples was measured from 4 hpi to 35 dpi using a Nanodrop spectrophotometer (Evans *et al*., 2012). The total chlorophyll content was calculated using the equation of Wellburn (1994): $Chl_{total} = 7{\cdot}12A_{664} + 18{\cdot}12A_{647}$

## RESULTS

*Sequencing and phylogeny analysis*

We used annotated family members of the gene of interest in arabidopsis and leguminous species in GenBank and other publicly available databases as query sequences to BLAST search our pea transcriptome data, and identified three *IPT*, three *LOG*, four *RR*, five *CKX*, four *CWINV*, four *SUT*, 15 *SWEET* and 13 *AAP* putative orthologous sequences in pea. Results of sequence verification via BLAST searching the GenBank database showed that most of the identified sequences were confirmed to be the target gene sequences. Phylogenetic analysis and gene family designations are shown in Supplementary Data Figs S1–S9. We have numbered both the *PsSWEET* gene family members and clades (Fig. S9) as outlined by Chandran (2015) and Eom *et al*. (2015), and not according to Patil *et al*. (2015) where gene families and clades are numbered somewhat differently.

*Morphological and microscopic differences are evident following inoculation with avirulent and virulent strains of* Rhodococcus fascians

The typical multiple shoot symptom of *R. fascians* infection was apparent at 5 dpi in plants inoculated with the virulent strain (vir-plants) (Fig. 1-1). By 9 dpi, 80–90 % of the vir-plants had multiple shoots branching at the crown region of the root and shoot, and root growth was less prolific when compared with plants inoculated with the avirulent strain (avir-plants) and the mock-inoculated control plants (con-plants). The reduced leaf expansion, stunted shoot growth with multiple shoots, shortened and thickened primary roots and suppressed lateral root growth were evident from 11 to 45 dpi in vir-plants (Fig. 1-1). By 38 dpi, most of the con-plants started flowering, some avir-plants had flowers but few vir-plants flowered. Leaf senescence was observed in con-plants and avir-plants from 40 dpi but not in the vir-plants. The avir-plants and con-plants had similar morphology throughout (Fig. 1-1).

A particularly noticeable response was that cotyledons on the vir-plants became bright green and remained robust throughout, compared with con-plants and avir-plants where the cotyledons were light yellow, becoming shrivelled and reduced in size as the plants grew (Fig. 1-3). The cotyledons inoculated with the virulent strain (vir-cots) showed increasing chlorophyll content from 11 dpi compared with the control (Fig. 1-4).

Light microscopy revealed early differences in infection of the seeds inoculated with either the virulent or the avirulent microbe (Fig. 1-2). Within 4 h of pea seeds being inoculated with the virulent strain 602, purple-stained *R. fascians* colonies were detectable in the intercellular spaces of the sub-epidermal layer of the seed coat (Fig. 1-2C), whereas bacteria were not detected in the seed coat of seeds inoculated with the avirulent strain 589 (avir-cot) (Fig. 1-2B). Within 2 dpi, virulent bacteria were present in the parenchyma layer of the seed coat (Fig. 1-2F) as well as on the surface of the cotyledon (Fig. 1-2I), whereas the avirulent strain of *R. fascians* was now detectable in the intercellular spaces of the sub-epidermal layer of the seed coat but not on the surface of the cotyledon (Fig. 1-2E, H). However, by 5 dpi, both strains of bacteria were spread across the surface of the cotyledon (Fig. 1-2K, L). By 15 dpi, the avirulent strain was evident as clumps of cells on the cotyledon surface (Fig. 1-2N). In comparison, the virulent strain appeared as a widespread accumulation of cells (Fig. 1-2O). Microscopically, increased colonization of the cotyledons by the virulent strain was apparent from 15 to 35 dpi (Fig. 1-2O, R), whereas colonization by the avirulent strain became more obvious in later stages of growth, mainly at 25 and 35 dpi (Fig. 1-2Q).

Scanning electron microscopy of the plant surfaces showed *R. fascians* present on cotyledons, roots, shoots and flower surfaces throughout the life cycle of the plant (Dhandapani, 2014).

*Endogenous cytokinins in inoculated pea tissues*

Peas imbibed in the presence of virulent and avirulent strains of *R. fascians* showed differential accumulation of cytokinins, in terms of both quantity and type (Table 1). Of the changes at the free base, riboside and nucleotide level, most noticeable were the strongly elevated levels of iP in the vir-cots relative to con-cots across all experimental time points. iPR levels were strongly increased in vir-cots at 4 hpi, but then fluctuated relative to con-cots. Both Z-type and iP-type cytokinins were significantly elevated in the avir-cots relative to the mock-inoculated controls, consistently at 15 and 25 dpi (Table 1).

Nucleotides were not detected in inoculated cotyledons at 4 hpi, but were generally decreased relative to controls at 2, 5 and 11 dpi in vir-cots, and generally elevated in avir-cots at 15 and 25 dpi (Table 1). The storage *O*-glucosyl forms were not detected in cotyledons until 5 dpi (Table 1). Both tZOG and tZROG were elevated in all vir-tissues at 5 dpi, but were decreased consistently subsequently relative to controls. In avir-cots the patterns were generally the opposite to those in vir-cots. The 7- and 9-glucoside conjugates of both *t*Z and iP were generally below the limit of detection. The *cis*-cytokinins and methyl-thio forms will be presented elsewhere. However, these forms did not correlate with virulence (data not shown).

*Expression of* RfIPT, RfLOG *and* RfCKX *genes during infection*

PCR confirmed that not only *IPT* and *CKX*, but also *LOG* is present in 18 virulent strains but not in 18 avirulent strains (Table S1). Primers were designed to discriminate between the pathogen genes and pea genes. Clear expression of the *R. fascians* genes was shown in cultures of the virulent strain (Fig. 2A). Following inoculation, expression of all three *R. fascians* genes was detected in the vir-cots but not in avir-cots. *RfIPT* was expressed strongly across time in the vir-cots. Expression of *RfLOG* was strongest in vir-cots at 5, 9 and 15 dpi, and that of *RfCKX* at 5 and 9 dpi (Fig. 2B).

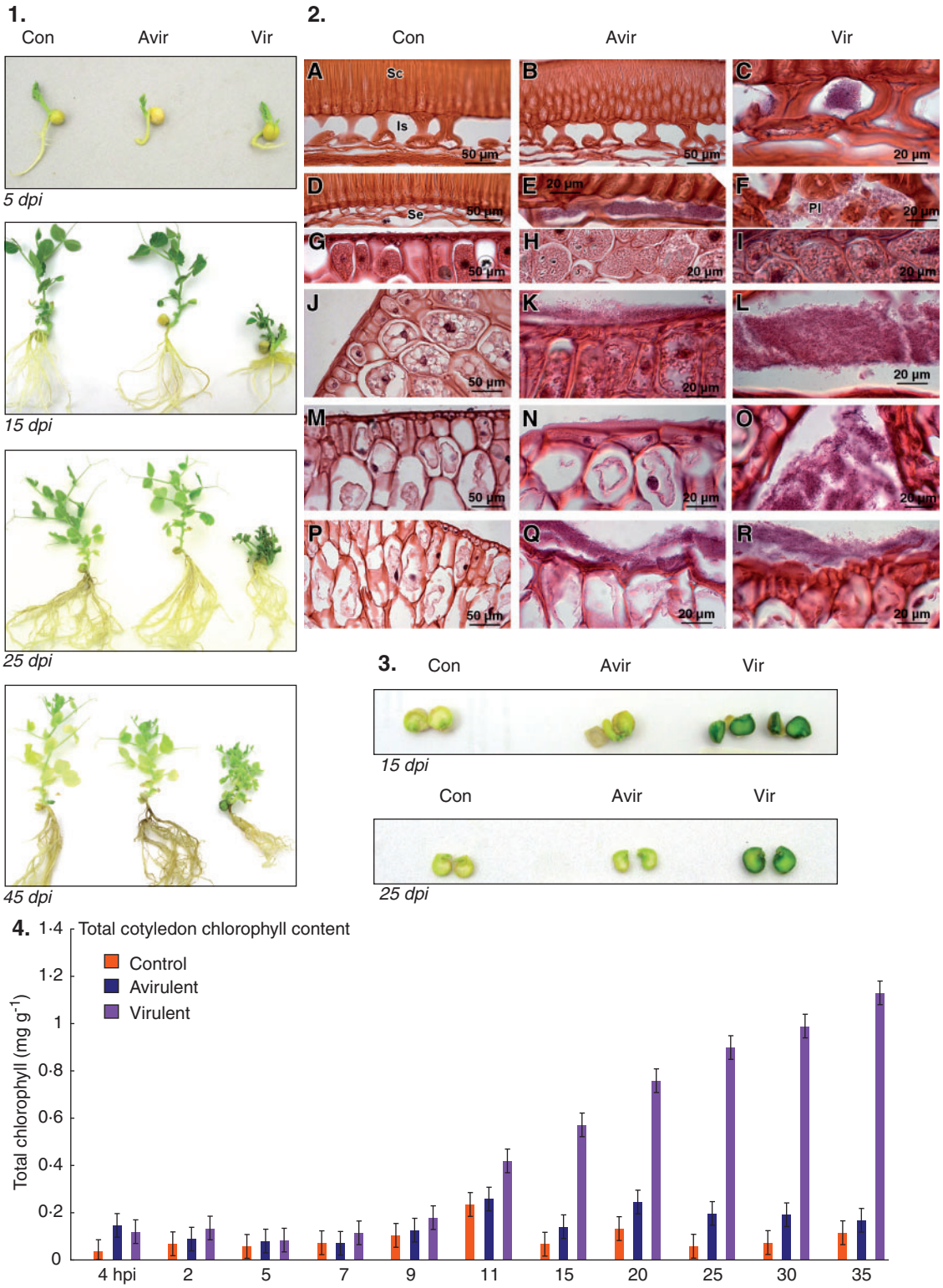


FIG. 1. Response of *Pisum sativum* following seed inoculation with *Rhodococcus fascians*. (1) Growth stages and morphology of *P. sativum* inoculated with *R. fascians* avirulent strain 589 (Avir), virulent strain 602 (Vir) and medium as mock inoculation (Con) grown in sterile agar containers at 5, 15, 25 and 45 days post-inoculation (dpi). (2) Light micrographs of sections of *P. sativum* seed coat and cotyledon following inoculation with *R. fascians* at 4 h post-inoculation (hpi) (A–C), 2 dpi (D–L), 5 dpi (J–L), 15 dpi (M–O) and 35 dpi (P–R). Sc, seed coat; Is, intercellular spaces in the seed coat; Se, sub-epidermal layer of the seed coat, and PL, parenchyma layer of the seed coat. Magnification for control (×40; 50 µm scale bar); magnification for *R. fascians*-inoculated tissues (×100; 20 µm scale bar). (3) Morphological differences between *P. sativum* cotyledons inoculated with *R. fascians* avirulent strain 589 (Avir), virulent strain 602 (Vir) and mock inoculated (Con) at 15 and 25 dpi. (4) Total chlorophyll content in cotyledons of *P. sativum* imbibed for 4 h with *R. fascians* avirulent strain 589 (Avirulent), virulent strain 602 (Virulent) and medium as mock inoculation (Control) grown in sterile agar containers until 35 dpi. The error bars are ± 1 s.d. of two biological replicates and four technical replicates.

TABLE 1. *Endogenous cytokinin content in* Pisum sativum *cotyledons following seed inoculation with* Rhodococcus fascians

| Cytokinin (pmol $g^{-1}$ d wt) | Time points | | | | | | | | | | | | | | | | | |
|---|---|---|---|---|---|---|---|---|---|---|---|---|---|---|---|---|---|---|
| | 4hpi | | | 2 dpi | | | 5 dpi | | | 11 dpi | | | 15 dpi | | | 25 dpi | | |
| Cotyledon | CON | AVIR | VIR | CON | AVIR | VIR | CON | AVIR | VIR | CON | AVIR | VIR | CON | AVIR | VIR | CON | AVIR | VIR |
| tZ | 1·65 | **3·08** | **2·79** | 5·26 | **2·76** | **2·14** | 1·89 | 2·27 | **1·00** | 2·26 | **1·56** | **0·61** | 0·65 | **1·26** | **1·13** | 1·04 | **1·6** | 0·8 |
| tZR | 0·13 | **0·09** | **0·1** | 1·01 | 1·16 | **0·44** | 0·33 | 0·4 | **0·18** | 0·34 | 0·16 | 0·04 | 0·28 | **0·18** | **0·13** | 0·16 | **1·03** | 0·15 |
| tZRMP | <LOD | <LOD | <LOD | 4·46 | 4·02 | **2·09** | 2·71 | 3·09 | 2·06 | 3·05 | 2·31 | **0·42** | 0·81 | 1·13 | **0·44** | 1·85 | 1·41 | **0·72** |
| tZOG | <LOD | <LOD | <LOD | <LOD | <LOD | <LOD | <LOD | **0·33** | 0·2 | 0·36 | **1·10** | **0·23** | 0·66 | 0·69 | 0·67 | 0·4 | **0·78** | **0·21** |
| tZROG | <LOD | <LOD | <LOD | 0·09 | 0·07 | 0·10 | 0·13 | **0·24** | **0·23** | 0·19 | **0·47** | **0·09** | 0·70 | 0·54 | 0·55 | 0·47 | **0·96** | **0·23** |
| iP | 1·66 | **3·75** | **4·15** | 1·76 | 1·74 | **7·59** | 1·61 | **1·93** | **3·44** | 2·28 | **3·29** | **11·95** | 1·39 | 1·86 | **7·93** | 2·22 | **4·54** | **14·92** |
| iPR | 0·22 | **3·41** | **11·66** | 1·52 | 1·03 | **2·33** | 1·32 | 0·92 | 1·01 | 0·96 | 1·15 | **0·51** | 0·89 | 1·97 | 1·92 | 0·82 | **3·27** | **1·73** |
| iPRMP | <LOD | <LOD | <LOD | 21·63 | 16·56 | **11·2** | 23·8 | 21·84 | **13·78** | 18·58 | **8·5** | **1·69** | 5·43 | **19·76** | **14·42** | 2·17 | **7·08** | 2·5 |

LOD, below detection limit; tZ7G, tZ9G, iP7G and iP9G were generally below the detection limits.
The pea seeds were imbibed for 4 h (hpi) with *R. fascians* strain 589 (AVIR), strain 602 (VIR) and with medium for mock inoculation (CON).
The data are averages of four biological replicates.
Numbers in bold indicate a significant difference from the control, $P < 0{\cdot}05$.

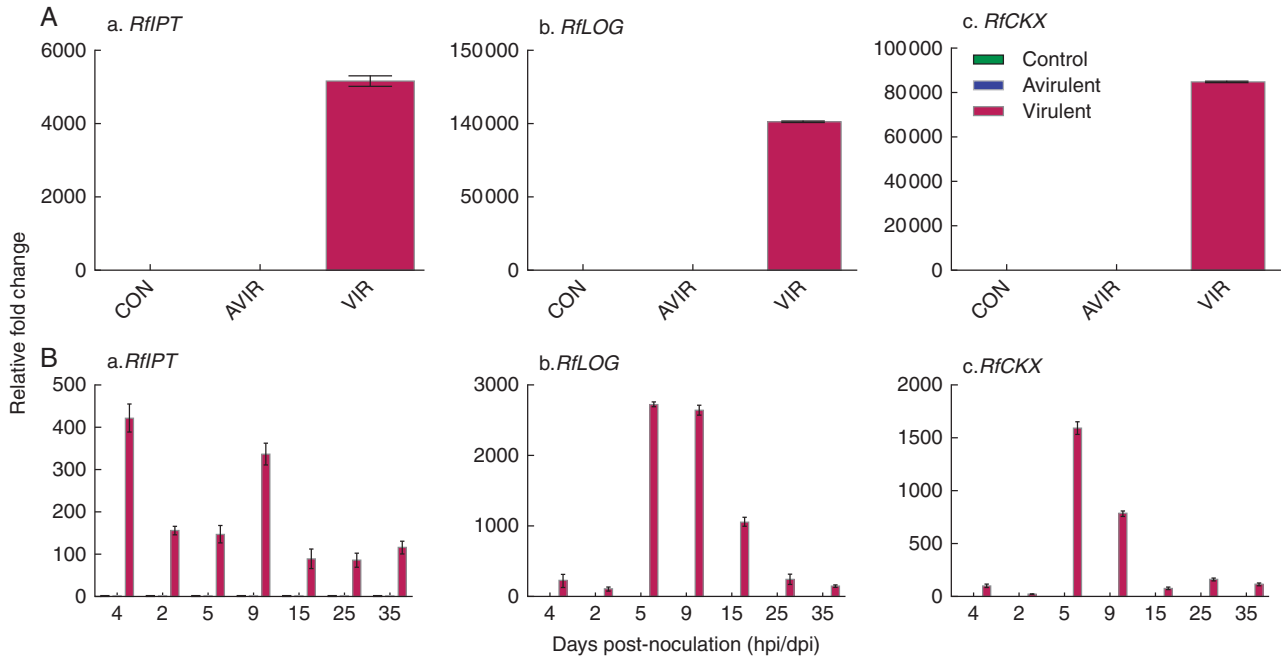


FIG. 2. Relative expression of *RfIPT*, *RfLOG* and *RfCKX* detected in *R. fascians* cultures and *Pisum sativum* cotyledons inoculated with *R. fascians*. (A) Expression of *RfIPT*, *RfLOG* and *RfCKX* was determined following RNA extraction and cDNA synthesis from *R. fascians* avirulent strain 589 (AVIR) and virulent strain 602 (VIR). A no-template reaction was used as control (CON). Relative fold change values were calculated using *Ps18S* as an internal control. The error bars are ± 1 s.d. using four technical replicates for each of two biological replicates in the RT–qPCR. (B) Following seed inoculation with *R. fascians* avirulent strain 589 (AVIR) and virulent strain 602 (VIR) from 4 h to 35 days post-inoculation. Relative fold change values were calculated using *PsEF*, *Ps18S*, *PsGAP* and *PsACT* as internal controls. The error bars are ± 1 s.d. using three technical replicates for each of two biological replicates in the RT–qPCR.

### *Expression of* PsIPT, PsLOG *and* PsCKX *genes in cotyledons inoculated with virulent* R. fascians

It would appear that virulent *R. fascians* and, to a lesser extent, the avirulent strain had an early effect on the expression of *PsIPT*, with all three gene family members showing enhanced expression within 4 hpi (Fig. 3). This was also shown in an independent experiment (Fig. S9). Subsequently, in the avir-cots there was a suppression of *PsIPT* expression until 25–35 dpi. By 2 dpi, in those plants inoculated with the virulent strain, *PsIPT* expression was reduced relative to the control, with the exception of *PsIPT2* at 9 and 15 dpi in cotyledons. Mirroring the *PsIPT* expression, *PsLOG* expression was elevated within 4 hpi in both vir- and avir-cots (Fig. 3). *PsLOG* expression then reduced in the avir-cots until the latter stages of the experiment. Conversely, *PsLOG8* was elevated in vir-cots at most growth stages.

With the exception of *PsCKX2*, the other four *PsCKX* gene family members showed elevated expression in both vir- and avir-cots within 4 hpi relative to controls, with expression in vir-cots exceeding that in avir-cots (Fig. 3). Throughout the experiment, various *PsCKX* gene family members showed elevated expression in vir-cots. *PsCKX1* and *PsCKX5* were mostly elevated in avir-cots at the later stages of the experiment. Increased *PsRR* activity relative to control was noticeable in

| Target genes | 4 hpi VIR | 2 dpi VIR | 5 dpi VIR | 9 dpi VIR | 15 dpi VIR | 25 dpi VIR | 35 dpi VIR | 4 hpi AVIR | 2 dpi AVIR | 5 dpi AVIR | 9 dpi AVIR | 15 dpi AVIR | 25 dpi AVIR | 35 dpi AVIR |
|---|---|---|---|---|---|---|---|---|---|---|---|---|---|---|
| *PsIPT1* | 6·9 | −2·3 | −3·2 | 1·6 | 1·5 | 1·6 | −1·1 | 2·8 | −8·1 | −7·8 | −2·4 | −1·1 | 5·8 | 2·4 |
| *PsIPT2* | 19·4 | −3·3 | 1·2 | 5·7 | 5·2 | −2·1 | −4·5 | 4·4 | −10·7 | −4·4 | −7·5 | −1·1 | −1·9 | −1·2 |
| *PsIPT4* | 24·6 | −1·9 | −3·9 | −5·0 | 3·7 | −4·6 | −2·3 | 5·8 | −10·8 | −12·5 | −27·1 | −4·4 | 5·0 | 1·7 |
| *PsLOG1* | 9·8 | −1·9 | −1·2 | 10·8 | 1·5 | 3·6 | 2·4 | 1·6 | −7·7 | −6·6 | −6·5 | 2·1 | 1·8 | 2·1 |
| *PsLOG6* | 84·8 | −5·8 | 5·1 | 1·7 | −2·1 | −2·0 | −1·2 | 21·0 | −13·7 | −6·9 | −2·8 | −2·1 | 1·5 | 3·3 |
| *PsLOG8* | 2·8 | −4·5 | 16·7 | 41·3 | 2·8 | 10·9 | 7·1 | 3·7 | −2·1 | −4·7 | −2·2 | −2·3 | 3·3 | 4·1 |
| *PsCKX1* | 15·5 | −2·2 | 9·6 | 2·7 | 1·2 | −1·0 | −3·5 | 3·3 | −2·2 | 1·1 | −1·3 | −1·3 | 6·0 | 3·3 |
| *PsCKX2* | −6·7 | −1·7 | −1·9 | −3·5 | 21·6 | 17·1 | 3·0 | −3·1 | −17·0 | −5·8 | −393·1 | 2·6 | 2·1 | −1·5 |
| *PsCKX3* | 15·0 | −3·3 | 23·1 | 8·8 | 2·0 | 8·1 | 6·1 | 4·2 | −7·8 | 2·1 | −2·0 | −3·0 | −2·4 | 3·5 |
| *PsCKX5* | 105·9 | 1·4 | −1·1 | 3·7 | 3·2 | 2·7 | 1·1 | 33·5 | −2·4 | −5·4 | −3·1 | −1·1 | 7·9 | 2·9 |
| *PsCKX7* | 80·0 | −1·8 | 2·7 | 2·8 | 1·9 | 2·1 | 3·4 | 5·8 | −5·4 | −4·3 | −2·2 | −2·4 | −1·9 | 1·8 |
| *PsRR3* | 33·2 | 1·3 | 17·4 | 29·2 | 6·4 | 5·9 | 2·0 | 3·9 | −1·0 | −9·4 | −3·3 | −2·7 | 3·5 | 3·5 |
| *PsRR5* | 25·1 | −1·3 | 58·2 | 89·4 | 2·5 | 5·5 | 25·5 | 3·9 | −4·8 | 1·7 | −1·8 | −21·4 | −2·0 | 8·4 |
| *PsRR6* | 76·2 | −1·7 | 4·3 | 9·6 | −2·2 | 1·0 | 3·7 | 1·0 | −2·4 | 1·5 | −2·4 | −3·3 | 16·5 | 17·7 |
| *PsRR9* | 10·2 | 2·0 | 3·3 | 60·8 | 3·4 | 11·7 | 8·0 | 2·3 | −1·2 | −25·4 | −4·6 | −4·8 | 6·0 | 11·0 |
| *PsAAP7a* (Cluster 1) | 2·0 | 1·3 | 73·8 | 23·7 | 0·4 | 29·6 | −3·1 | −25·1 | −10·1 | 1·9 | 1·9 | −6·5 | −3·6 | 3·8 |
| *PsAAP7b* | 13·3 | −2·9 | 2·8 | 3·9 | −1·5 | 1·7 | −1·6 | 2·0 | −6·1 | −2·5 | −1·6 | −1·3 | 16·2 | 3·9 |
| *PsAAP7c* | 84·7 | 5·6 | 31·7 | 1·4 | 2·7 | 1·6 | 2·4 | 8·3 | −10·1 | −1·5 | −7·4 | −4·7 | 13·1 | 6·8 |
| *PsAAP2a* (Cluster 3A) | 103·9 | −9·6 | 103·7 | 11·8 | 1·2 | 1·3 | 2·9 | 2·8 | −13·3 | 2·8 | −1·0 | −1·1 | 2·7 | 13·8 |
| *PsAAP2b* | −2·0 | −2·9 | 2·2 | 2·8 | −1·3 | −2·0 | 1·9 | −3·0 | −6·9 | −9·8 | −2·5 | −2·9 | 2·4 | 7·0 |
| *PsAAP2c* | 55·0 | −2·8 | 41·0 | 14·1 | 1·5 | 1·2 | 1·1 | 7·3 | −5·6 | 1·2 | 1·5 | 1·1 | 4·3 | 7·6 |
| *PsAAP2d* | 1·1 | −3·7 | 17·9 | 6·5 | −1·4 | −2·5 | −1·1 | −3·1 | −6·2 | 5·3 | −1·6 | −2·3 | 3·1 | 5·8 |
| *PsAAP3a* | 1·8 | 1·5 | 15·5 | 4·3 | −4·1 | −3·0 | 1·4 | −9·2 | −3·6 | −1·0 | 1·2 | −1·1 | 9·0 | 5·9 |
| *PsAAP3b* | 7·5 | −1·9 | 5·0 | 2·1 | −1·3 | −1·8 | 1·6 | 3·6 | 1·3 | 3·3 | 1·4 | 3·5 | 7·8 | 4·1 |
| *PsAAP1* (Cluster 4B) | 7·3 | −5·4 | 74·9 | 12·6 | 1·0 | 1·1 | 1·2 | 7·4 | 1·0 | 2·8 | −1·4 | 1·3 | 4·7 | 3·8 |
| *PsAAP6a* | −1·1 | −4·3 | 2·1 | 12·4 | 4·5 | 1·2 | 2·4 | −1·5 | −3·2 | −28·4 | −13·3 | 0·8 | 1·1 | 5·8 |
| *PsAAP6b* | 3·5 | −2·7 | 4·6 | 4·9 | 2·0 | −2·1 | −2·0 | 1·3 | −1·1 | −45·2 | −1·0 | −1·4 | 9·5 | 5·2 |
| *PsAAP8* | 10·4 | −7·1 | 2·1 | 12·4 | 7·2 | −1·2 | 2·9 | 2·8 | −35·1 | −33·0 | −3·2 | 1·6 | 3·0 | 6·2 |
| *PsSUT1* | 8·5 | −2·6 | 2·0 | 3·2 | −1·5 | 1·5 | 0·9 | 2·7 | −4·8 | −11·6 | −1·7 | −1·1 | 4·2 | 3·1 |
| *PsSUT2* | 2·8 | −3·1 | 7·5 | 3·7 | 1·9 | 2·4 | 2·9 | 1·1 | −15·9 | −1·4 | −2·8 | −2·5 | 3·9 | 5·6 |
| *PsSUT5* | 6·7 | −6·3 | 3·4 | 15·5 | 4·4 | 3·9 | 2·1 | 2·7 | −33·2 | −6·8 | −4·2 | 1·1 | 5·3 | 4·0 |
| *PsSUT3* | 7·1 | −3·6 | 17·3 | 28·3 | 4·5 | 1·8 | 15·4 | 3·5 | −5·3 | −3·4 | −2·1 | −2·1 | 2·9 | 9·2 |
| *PsCWINV1* | 100·2 | −4·6 | 43·3 | 72·8 | 152·6 | 18·6 | 12·9 | 7·1 | −6·4 | −13·6 | −14·3 | −1·3 | 8·8 | 11·7 |
| *PsCWINV2* | −1·3 | 1·2 | 65·0 | 44·6 | −15·2 | −5·4 | 1·4 | −14·6 | −1·5 | −1·7 | −1·8 | −40·2 | 1·1 | 6·3 |
| *PsCWINV3* | 12·2 | −3·6 | 22·2 | 195·0 | 63·2 | 7·4 | 20·8 | 10·6 | −11·0 | −3·1 | −10·9 | −4·4 | 6·1 | 3·4 |
| *PsCWINV6* | −1·2 | 7·5 | 2·6 | 2·3 | −1·1 | 2·0 | 2·9 | −4·1 | −3·5 | −2·0 | −1·9 | 1·3 | 7·8 | 11·6 |
| *PsSW1* (Clade I) | 5·3 | −2·4 | 3·2 | 2·9 | 1·1 | 1·1 | 3·8 | 1·3 | −1·3 | −2·5 | −1·3 | 4·7 | 6·1 | 6·2 |
| *PsSW2a* | 6591·1 | 2140·3 | 1598·6 | 6384·9 | 1194·9 | 1761·3 | 1278·3 | 2·5 | −1·7 | −2·4 | −1·3 | 2·8 | 3·2 | 3·4 |
| *PsSW2b* | 2·3 | −4·5 | 1·2 | 2·0 | −9·5 | −3·9 | 8·1 | −3·5 | −4·4 | −6·9 | −1·5 | −3·8 | 1·6 | 58·3 |
| *PsSW4* (Clade II) | 84·3 | 3·2 | 21·6 | 19·6 | 1·5 | 3·5 | 1·5 | 44·4 | −12·5 | −4·8 | −1·7 | −5·6 | 18·3 | 7·8 |
| *PsSW5a* | 1·4 | −3·8 | 15·5 | 11·6 | 6·4 | 1·3 | 3·1 | 1·0 | −16·8 | −4·2 | 2·7 | −1·5 | 14·4 | 10·4 |
| *PsSW5b* | 2·6 | −2·3 | 3·3 | 9·6 | 6·8 | 3·1 | 4·0 | 1·7 | −5·9 | −6·1 | −2·3 | 1·2 | 4·4 | 2·2 |
| *PsSW7* | 6·7 | −1·7 | 22·8 | 59·2 | 48·1 | 7·5 | 29·0 | 3·6 | 2·0 | −16·1 | −5·3 | 1·1 | 2·6 | 11·3 |
| *PsSW9* (Clade III) | −2·4 | 2·0 | 1·2 | 5·4 | 1·2 | 1·2 | 1·3 | −3·9 | 2·5 | −9·6 | −5·8 | 1·2 | 1·3 | 2·5 |
| *PsSW12* | −1·2 | −3·6 | 2·4 | 3·1 | 1·9 | 1·2 | −1·5 | −14·6 | −1·3 | −2·6 | −1·3 | 5·2 | 9·5 | 4·2 |
| *PsSW13* | 1·1 | −7·1 | 2·3 | −1·0 | 1·0 | −6·1 | −2·8 | 1411·3 | 5433·0 | 2723·6 | 8628·9 | 2589·3 | 2229·8 | 4465·5 |
| *PsSW15a* | 10·9 | 1·7 | 59·4 | 25·5 | 5·6 | 5·1 | 17·2 | 4·1 | 5·9 | 2·4 | −3·0 | −23·0 | 2·6 | 25·6 |
| *PsSW15b* | 106·9 | −20·9 | 728·8 | 187·2 | 325·6 | 33·0 | 425·5 | 4·3 | −1·6 | −4·0 | −7·4 | −1·6 | 35·2 | 39·2 |
| *PsSW15c* | 21·7 | −4·3 | −2·1 | 10·3 | 7·1 | 6·6 | 24·8 | 5·3 | −45·7 | −246·1 | −9·8 | −50·7 | 5·3 | 1·7 |
| *PsSW15d* | −2·9 | −1·7 | 10·3 | 78·0 | 23·6 | 11·6 | 125·3 | 1·1 | 1·4 | −8·9 | −2·7 | −35·3 | 1·4 | 140·4 |
| *PsSW17* (Clade IV) | 2·1 | −5·3 | 1·3 | 10·8 | 4·9 | 1·6 | 8·8 | 2·4 | −1·9 | −10·5 | 1·4 | −2·1 | 20·9 | 4·2 |

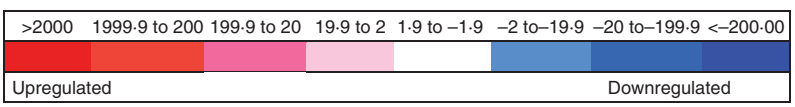


FIG. 3. Relative expression of cytokinin biosynthesis (*PsIPT*), degradation (*PsCKX*) and response regulator (*PsRR*) gene family members along with *PsAAP*, *PsSUT*, *PsCWINV* and *PsSWEET* gene family members in *Pisum sativum* cotyledons following seed inoculation with *Rhodococcus fascians* strain 589 (AVIR) and virulent strain 602 (VIR) from 4 h to 35 d post-inoculation. Values are fold changes relative to the expression of the mock-inoculated control. Initial fold change values were calculated using *PsEF*, *Ps18S*, *PsGAP* and *PsACT* as internal controls using three technical replicates for each of two biological replicates in the RT–qPCR. The relative expression level of each gene was then compared with the expression in pea cotyledons inoculated with medium as the mock-inoculated control. The colour scale indicates upregulated expression (red scale), similar (white) and downregulated expression (blue scale) relative to the mock-inoculated control.

vir-cots throughout the experiment, but particularly at 4 hpi and at 5 and 9 dpi (Fig. 3). Expression of several *PsRR* genes was elevated at 25 and 35 dpi in avir-cots.

### *Expression of amino acid transporters in inoculated pea tissues*

Relative to control, enhanced expression of several of the *PsAAP* gene family members was apparent in vir-cots at 4 hpi (Fig. 3). Most noticeable was enhanced expression at 5 and 9 dpi and the subsequent lesser expression of most *PsAAP* gene family members over time in vir-cots. In contrast, elevated expression of *PsAAP* gene family members relative to controls was consistently shown in avir-cots at 25 and 35 dpi.

### *Expression of sugar transporters in inoculated pea tissues*

With the exception of vir-cots at 2 dpi, expression of Type I *PsSUT5* and *PsSUT2*, and Type II *PsSUT3* was enhanced in vir-cots relative to controls throughout the experiment (Fig. 3). Enhanced expression of this gene family relative to controls was apparent in avir-cots at 4 hpi, but decreased expression relative to controls then occurred from 2 to 9 dpi. Enhanced expression was evident in avir-cots at 25 and 35 dpi.

### *Expression of multiple* PsSWEET *gene family members in inoculated pea tissues*

Constitutively strong expression was shown for *PsSW2a*, a Clade I *SWEET*, in vir-cots (Fig. 3). Transcript levels of three of the four Clade II members (*PsSW4*, *5b* and *7*) were elevated at 4 hpi, but not relative to controls at 2 dpi, but were subsequently elevated through to 35 dpi. Several of the Clade III SWEETs in vir-cots, particularly *PsSW15a*, *b* and *d*, were elevated relative to the control throughout development. Strong constitutive expression of Clade III *PsSW13* was detected in avir-cots from 4 hpi to 35 dpi (Fig. 3). Additionally, several other Clade III *SWEET* genes that were expressed at 4 hpi were expressed more strongly at 25 and/or 35 dpi in the avir-cots.

### *Expression of cell wall invertases in inoculated pea tissues*

Strong expression of *PsCWINV1* and *PsCWINV3* was seen in vir-cots at all time points; and in *PsCWINV2* at 5 and 9 dpi (Fig. 3). Interestingly, increased expression relative to the control was observed for *PsCWINV1* and *PsCWINV3* gene family members in avir-cots at 4 hpi and for most family members at 25 and 35 dpi.

## DISCUSSION

### *Infection by virulent* R. fascians *leads to retention and greening of cotyledons*

The marked increase in chlorophyll content of the cotyledons infected by the virulent strain was particularly striking, but not apparent until several days after the appearance of multiple shoots. Cornelis *et al.* (2001) observed the colonizing behaviour of both D188 and its plasmid-cured strain (D188-5) on both tobacco and arabidopsis seedlings. They suggested that both strains colonized the plant surface extensively and increasingly over time, but with less penetration of cell layers by D188-5 compared with D188 in infected tobacco. Our wild-type virulent strain spread through the seed coat and onto the surface of cotyledons faster than the wild-type avirulent strain, and was clearly visible prior to symptom emergence. There was not strong evidence for penetration of the bacteria beyond the surface layer of cells.

Previously Depudyt *et al.* (2008, 2009) had shown, in arabidopsis, decreased expression of *AtIPT* (particularly *AtIPT7*), increased *AtCKX* and increased *AtRR* expression relative to D188-5. They also reported an early increase in iPRMP and iP. We compared expression of both a virulent and an avirulent strain with mock-inoculated controls within 4 h of inoculation, and showed, relative to the mock-inoculated control, that *PsIPT* gene family members were initially strongly up-regulated in both vir- and avir-cots. This is reflected in the elevated levels of iP, iPR and *t*Z in the cotyledons. Matching this was strong expression of the cytokinin *PsRR* genes, and also of *PsCKX* expression. Interestingly, increased activity of the enzymes of the isoprenoid pathway has been reported during the initial 2–6 h of imbibition (Green and Baisted, 1972), indicating that a supply of precursor was probably available to the *PsIPT* and *RfIPT* genes. An early and transient expression of *BrIPT* genes was also noted by Ando *et al.* (2005) during clubroot infection in Chinese cabbage. They suggested that this transient induction of *BrIPT* expression may be the 'trigger for clubroot development'. Potentially, then, the early upregulation of *PsIPT* is indicative of recognition by the plant of the presence of the bacteria, irrespective of pathogenic status.

However, subsequently, *PsIPT* expression was depressed in both vir- and avir-cots. As the iP levels in the vir-cots continued to be greater than in the controls, the source of the iP in the vir-cots was now likely to be from the *RfIPT*. At the stage when the increased chlorophyll levels were apparent (11 dpi), iPRMP and ZRMP levels were actually less than in the con-cots, and less than in the avir-cots, reflecting earlier results obtained in pea (Eason *et al.*, 1996) and arabidopsis (Depuydt *et al.*, 2008). However, the expression of *RfLOG* and the elevated expression of *PsLOG8* are likely to account for the low level of nucleotides in the vir-cots. The elevated expression of the *PsRR* genes in the vir-cots is indicative of active signal transduction (Hwang *et al.*, 2012), and the elevated *PsCKX* expression is indicative of the plant homeostatic mechanisms coming into play – albeit somewhat ineffectually – a situation similar to that occurring in arabidopsis leaves responding to *R. fascians* D188 (Depudyt *et al.*, 2008; Pertry *et al.*, 2009).

### *Virulent and avirulent* R. fascians *strains cause changes in expression of genes regulating source–sink dynamics*

As evident in the heat map (Fig. 3), infection by the virulent strain had a marked effect on expression of *PsCWINV*, *PsSUT* and *SWEET* genes – key components in the regulation of source–sink dynamics. Additionally, we showed early changes in gene expression by the plant in response to the avirulent bacterium and consistently after some 25 and 35 dpi, by which time epiphytic colonies were well established.

Depuydt *et al*. (2009) reported that within 4 dpi, well before symptoms were apparent, *AtCWINV* was induced by both D188 and D188-5, but enzyme activity was greater and lasted longer following infection by D188. Enhanced expression of *PsCWINV* genes was particularly noticeable in the vir-cots. Further supporting the establishment of a carbohydrate sink for the bacteria is the upregulation of sucrose transporter genes. Moreover, strong expression of *SWEET* gene family members was also evident. However, in this case, the *SWEET* gene family members may have had opposite effects: Clade I AtSWEET2 transports glucose to the vacuole (Chen 2015) and *PsSW2a*, a Clade I *SWEET*, was elevated in response to the virulent strain. This aligns with the suggestion by Chen *et al*. (2015) that expression in the roots of *AtSWEET2* restricted the amount of glucose in the apoplast, by sequestering it to the vacuole. In the case of *R. fascians*, expression of several Clade II and III *SWEET* genes was also elevated in vir-cots, in which case hexoses and sucrose would have been exported to the apoplasm. These sugars have been detected in tissues of arabidopsis infected with the virulent D188 strain (Depuydt *et al*., 2009). As sugars have recently been identified as key components of the release of apical dominance (Barbier *et al*., 2015), a high sugar environment may be the signal for multiple bud formation, as suggested for witches' broom disease of cacao (Barau *et al*., 2015).

In contrast, *PsSW13*, a Clade III *SWEET*, was strongly upregulated in avir-cots, but not in vir-cots. Additionally, several *PsCWINV* and *PsSUT* gene family members were also upregulated later in development, supporting the contention that the epiphytic bacteria are also impacting on metabolism (Depuydt *et al*., 2009). Along with establishing a carbon supply, a supply of amino acids was secured by the virulent bacterium through upregulation of *PsAAP* genes in the germinating seeds. However, and particularly later in the experiment, the epiphytic colonies also impacted on amino acid transporters.

Our data add to the earlier arabidopsis microarray analysis by Depuydt *et al*. (2009) which revealed not only that D188 infection modulated primary metabolism, but also that inoculation by the avirulent D188-5 caused changes relative to the mock-inoculated control. However, our data provide an interesting time component, with both virulent and avirulent strains impacting plant gene expression early during inoculation. The apparent decrease in impact of the bacteria at 2 dpi may reflect the transition in the cotyledons from the initial metabolism occurring during Phase I imbibition and the mobilization of reserves in the germinating seedling by 2 dpi, when the radicle and plumule were emerging (Weitbrecht *et al*., 2011). Clearly, plant cytokinin homeostasis and sink metabolism were then affected strongly by the virulent strain, with the avirulent strain impacting more modestly later in the experiment as the cotyledon reserves were becoming depleted.

## CONCLUSIONS

In conclusion, it is clear that both the virulent and avirulent strains affected the expression of genes involved in the transport of carbon and nitrogen, as well as cytokinin biosynthesis and metabolism. Only the virulent strain markedly impacted both morphogenesis and the integrity of the cotyledon. We suggest that the interaction between cytokinins, *PsCWINV* and *PsSWEET* genes contributes to the loss of apical dominance and the appearance of multiple shoots emerging from the seeds inoculated with the virulent bacterium, as well as the re-greening and maintenance of the cotyledon.

However, whether the elevated iP alone is sufficient to have such a marked impact on the plant is yet to be determined. Subsequent investigations will focus on expression of *RfMT1* and *RfMT2* and levels of methylated cytokinins [newly identified from *Rhodococcus*-infected plant tissues by Radhika *et al*. (2015)], as well as the methylthio- and *cis*-forms of the cytokinins. We will then be able to compare, in pea, the impact of the methylated cytokinins (Radhika *et al*., 2015), with the 'trick-with-the-mix' hypothesis developed based on experiments with *R. fascians* and arabidopsis (Pertry *et al*., 2009, 2010), with the suggestion by Creason *et al*. (2014) that only one cytokinin type (the iP-type) is necessary for disease symptoms to be manifested.

## SUPPLEMENTARY DATA

Supplementary data are available online at www.aob.oxfordjournals.org and consist of the following. Figure S1: phylogenetic tree of *IPT*. Figure S2: phylogenetic tree of *LOG*. Figure S3: phylogenetic tree of *CKX*. Figure S4: phylogenetic tree of *RR*. Figure S5: phylogenetic tree of *SUT*. Figure S6: phylogenetic tree of *CWINV/INV*. Figure S7: phylogenetic tree of *AAP*. Figure S8: phylogenetic tree of *SWEET*. Figure S9: *PsIPT*, *PsLOG*, *PsCKX* and *PsRR* expression in seeds of *P. sativum* following seed inoculation with *R. fascians* at 4 h and 2 days post-inoculation. Table S1: PCR detection of *RfIPT*, *RfLOG* and *RfCKX* genes in *R. fascians* cultures. Table S2: primer sequences used for RT–qPCR, and GenBank accession numbers.

## ACKNOWLEDGEMENTS

A UC doctoral scholarship to P.D. is gratefully acknowledged. Thanks to Graeme Bull and Jan McKenzie for histological specimen preparation and light microscopy; Neil Andrews for assisting in preparation and operation of the scanning electron microscope; Hana Martinková and Ivan Petřík for help with cytokinin analyses; Annu Smitha Ninan for isolating some of the transporter gene family members; and Matt Walters for assistance in graphic presentation. The constructive advice from the two anonymous referees is acknowledged with thanks. O.N. was funded by the Ministry of Education, Youth and Sports of the Czech Republic (the National Program for Sustainability I Nr. LO1204) and the "Navrat" program (LK21306).

## REFERENCES

**Ando S, Asano T, Tsushima S, Kamachi S, Hagio T, Tabei Y. 2005.** Changes in gene expression of putative isopentenyltransferase during clubroot development in Chinese cabbage (*Brassica rapa* L.). *Physiological and Molecular Plant Pathology* **67**: 59–67.

**Antoniadi I, Plačková L, Simonovik B, *et al.* 2015.** Cell-type specific cytokinin distribution within the Arabidopsis primary root apex. *The Plant Cell* **27**: 1955–1967.

**Albacete A, Cantero-Navarro E, Großkinsky DK, *et al.* 2015.** Ectopic overexpression of the cell wall invertase gene *CIN1* leads to dehydration avoidance in tomato. *Journal of Experimental Botany* **66**: 863–878.

**Balibrea Lara ME, Gonzalez Garcia M-C, Fatima T, *et al.* 2004.** Extracellular invertase is an essential component of cytokinin-mediated delay of senescence. *The Plant Cell* **16**: 1276–1287.

**Barau J, Grandis A, Carvalho VMdA, *et al.* 2015.** Apoplastic and intracellular plant sugars regulate developmental transitions in witches' broom disease of cacao. *Journal of Experimental Botany* **66**: 1325–1337.

**Barbier FF, Lunn JE, Beveridge CA. 2015.** Ready, steady, go! A sugar hit starts the race to shoot branching. *Current Opinion in Plant Biology* **25**: 39–45.

**Berger S, Sinha AK, Roitsch T. 2007.** Plant physiology meets phytopathology: plant primary metabolism and plant–pathogen interactions. *Journal of Experimental Botany* **58**: 4019–4026.

**Bustin SA, Benes V, Garson JA, *et al.* 2009.** The MIQE guidelines: minimum information for publication of quantitative real-time PCR experiments. *Clinical Chemistry* **55**: 611–622.

**Carletom HM, Druvy RAB. 1957.** *Histological technique for normal pathological tissues and the identification of parasites*, 3rd edn. London: Oxford University Press.

**Chandran D. 2015.** Co-option of developmentally regulated plant *SWEET* transporters for pathogen nutrition and abiotic stress tolerance. *IUBMB Life* **67**: 461–71.

**Chandran D, Inada N, Hather G, Kleindt CK, Wildermuth MC. 2010.** Laser microdissection of Arabidopsis cells at the powdery mildew infection site reveals site-specific processes and regulators. *Proceedings of the National Academy of Sciences, USA* **107**: 460–465.

**Chen H-Y, Huh J-H, Yu Y-C, *et al.* 2015.** The *Arabidopsis* vacuolar sugar transporter *SWEET2* limits carbon sequestration from roots and restricts *Pythium* infection. *The Plant Journal* **83**: 1046–1058.

**Chen L-Q, Hou B-H, Lalonde S, *et al.* 2010.** Sugar transporters for intercellular exchange and nutrition of pathogens. *Nature* **468**: 527–532.

**Chen L-Q, Qu XQ, Hou B-H, *et al.* 2012.** Sucrose efflux mediated by SWEET proteins as a key step for phloem transport. *Science* **335**: 207–211.

**Cornelis K, Ritsema T, Nijsse J, Holsters M, Goethals K, Jaziri M. 2001.** The plant pathogen *Rhodococcus fascians* colonizes the exterior and interior of the aerial parts of plants. *Molecular Plant-Microbe Interactions* **14**: 599–608.

**Creason AL, Vandeputte OM, Savory EA, *et al.* 2014.** Analysis of genome sequences from plant pathogenic *Rhodococcus* reveals genetic novelties in virulence loci. *PLoS One* **9**: e101996.

**Depuydt S, Doležal K, Van Lijsebettens M, Moritz T, Holsters M, Vereecke D. 2008.** Modulation of the hormone setting by *Rhodococcus fascians* results in ectopic KNOX activation in *Arabidopsis*. *Plant Physiology* **146**: 1267–1281.

**Depuydt S, Tenkamp S, Fernie AR, *et al.* 2009.** An integrated genomics approach to define niche establishment by *Rhodococcus fascians*. *Plant Physiology* **149**: 1366–1386.

**Derveaux S, Vandesompele J, Hellemans J. 2010.** How to do successful gene expression analysis using real-time PCR. *Methods* **50**: 227–230.

**Dhandapani P. 2014.** *Rhodococcus fascians–plant interactions: microbiological and molecular aspects*. PhD Thesis, University of Canterbury, New Zealand.

**Dobrev PI, Kamínek M. 2002.** Fast and efficient separation of cytokinins from auxin and abscisic acid and their purification using mixed-mode solid-phase extraction. *Journal of Chromatography A* **950**: 21–29.

**Eason JR, Jameson PE, Bannister P. 1995.** Virulence assessment of *Rhodococcus fascians* strains on pea cultivars. *Plant Pathology* **44**: 141–147.

**Eason JR, Morris RO, Jameson PE. 1996.** The relationship between virulence and cytokinin production by *Rhodococcus fascians* (Tilford 1936) Goodfellow 1984. *Plant Pathology* **45**: 323–331.

**Ehness R, Ecker M, Godt DE, Roitsch T. 1997.** Glucose and stress independently regulate source and sink metabolism and defense mechanisms via signal transduction pathways involving protein phosphorylation. *The Plant Cell* **9**: 1825–1841.

**Ehneß R, Roitsch T. 1997.** Co-ordinated induction of mRNAs for extracellular invertase and a glucose transporter in *Chenopodium rubrum* by cytokinins. *The Plant Journal* **11**: 539–548.

**Eom JS, Chen LQ, Sosso D, *et al.* 2015.** SWEETs, transporters for intracellular and intercellular sugar translocation. *Current Opinion in Plant Biology* **25**: 53–62.

**Evans T, Song J, Jameson PE. 2012.** Micro-scale chlorophyll analysis and developmental expression of a cytokinin oxidase/dehydrogenase gene during leaf development and senescence. *Plant Growth Regulation* **66**: 95–99.

**Fagard M, Launay A, Clément G, *et al.* 2014.** Nitrogen metabolism meets phytopathology. *Journal of Experimental Botany* **65**: 5643–5656.

**Francis IM, Stes E, Zhang Y, Rangel D, Audenaert K, Vereecke D. 2016.** Mining the genome of *Rhodococcus fascians*, a plant growth-promoting bacterium gone astray. *New Biotechnology* (in press).

**Galis I, Bilyeu K, Wood G, Jameson PE. 2005.** *Rhodococcus fascians*: shoot proliferation without elevated cytokinins? *Plant Growth Regulation* **46**: 109–115.

**Green TR, Baisted DJ. 1972.** Development of the activities of enzymes of the isoprenoid pathway during early stages of pea-seed germination. *Biochemical Journal* **130**: 983–995.

**Großkinsky DK, Naseem M, Abdelmohsen UR, *et al.* 2011.** Cytokinins mediate resistance against *Pseudomonas syringae* in tobacco through increased antimicrobial phytoalexin synthesis independent of salicylic acid signaling. *Plant Physiology* **157**: 815–830.

**Guo WJ, Nagy R, Chen HY, *et al.* 2014.** SWEET17, a facilitative transporter, mediates fructose transport across the tonoplast of *Arabidopsis* roots and leaves. *Plant Physiology* **164**: 777–789.

**Gutierrez L, Mauriat M, Pelloux J, Bellini C, Van Wuytswinkel O. 2008.** Towards a systematic validation of references in real-time RT–PCR. *The Plant Cell* **20**: 1734–1735.

**Hwang I, Sheen J, Muller B. 2012.** Cytokinin signaling networks. *Annual Review of Plant Biology* **63**: 353–380.

**Jameson PE. 2000.** Cytokinins and auxins in plant–pathogen interactions – an overview. *Plant Growth Regulation* **32**: 369–380.

**Jameson PE. 2017.** Cytokinins. In: Thomas B, Murray B, Murphy DJ, eds. *Encyclopedia of applied plant sciences*, Vol **1**. Waltham, MA: Academic Press, pp. 391-402.

**Jameson PE, Song J. 2016.** Cytokinin: a key driver of seed yield. *Journal of Experimental Botany* **67**: 593–606.

**Kado CI, Heskett MG. 1970.** Selective media for isolation of *Agrobacterium*, *Corynebacterium*, *Erwinia*, *Pseudomonas* and *Xanthomonas*. *Phytopatholoy* **60**: 969–976.

**Kitin P, Iliev I, Scaltsoyiannes A, Nellas C, Rubos A, Funada R. 2005.** A comparative histological study between normal and fasciated shoots of *Prunus avium* generated *in vitro*. *Plant Cell, Tissue and Organ Culture* **82**: 141–150.

**Lacey MS. 1936.** Studies in bacteriosis. XXII. 1. Isolation of a bacterium associated with 'fasciaton' of sweet peas, 'cauliflower' strawberry plants and 'leafy gall' of various plants. *Annals of Applied Biology* **23**: 302–310.

**Lawson E, Gantotti B, Starr M. 1982.** A 78-megadalton plasmid occurs in avirulent strains as well as virulent strains of *Corynebacterium fascians*. *Current Microbiology* **7**: 327–332.

**Li T, Huang S, Zhou J, Yang B. 2013.** Designer TAL effectors induce disease susceptibility and resistance to *Xanthomonas oryzae* pv. *oryzae* in rice. *Molecular Plant* **6**: 781–789.

**Lomin SN, Krivosheev DM, Steklov MY, *et al.* 2015.** Plant membrane assays with cytokinin receptors underpin the unique role of free cytokinin bases as biologically active ligands. *Journal of Experimental Botany* **66**: 1851–1863.

**Mothes K, Engelbrecht L. 1963.** On the activity of a kinetin-like root factor. *Life Sciences* **2**: 852–857.

**Nandi S, Palni L. 1989.** Transport and metabolism of dihydrozeatin riboside in germinating lupin seeds. *Journal of Experimental Botany* **40**: 615–621.

**Nandi S, Palni L, Letham D, Knypl J. 1988.** The biosynthesis of cytokinins in germinating lupin seeds. *Journal of Experimental Botany* **39**: 1649–1665.

**Nawa Y, Asahi T. 1971.** Rapid development of mitichondria in pea cotyledons during early stage of germination. *Plant Physiology* **48**: 671–674.

**Patil G, Valliyodan B, Deshmukh R, *et al.* 2015.** Soybean (*Glycine max*) *SWEET* gene family: insights through comparative genomics, transcriptome profiling and whole genome re-sequence analysis. *BMC Genomics* **16**: 520.

**Pertry I, Václavíková K, Depuydt S, *et al.* 2009.** Identification of *Rhodococcus fascians* cytokinins and their modus operandi to reshape the plant. *Proceedings of the National Academy of Sciences, USA* **106**: 929–934.

**Pertry I, Václavíková K, Gemrotová M, *et al.* 2010.** *Rhodococcus fascians* impacts plant development through the dynamic fas-mediated production of a cytokinin mix. *Molecular Plant-Microbe Interactions* **23**: 1164–1174.

**Pfaffl M, Hageleit M. 2001.** Validities of mRNA quantification using recombinant RNA and recombinant DNA external calibration curves in real-time RT–PCR. *Biotechnology Letters* **23**: 275–282.

**Pratelli R, Pilot G. 2014.** Regulation of amino acid metabolic enzymes and transporters in plants. *Journal of Experimental Botany* **65**: 5535–5556.

**Radhika V, Ueda N, Tsuboi Y, *et al.* 2015.** Methylated cytokinins from the phytopathogen *Rhodococcus fascians* mimic plant hormone activity. *Plant Physiology* **169**: 1118–1126.

**Roitsch T, Gonzalez MC. 2004.** Function and regulation of plant invertases: sweet sensations. *Trends in Plant Science* **9**: 606–613.

**Siemens J, Gonzalez MC, Wolf S, *et al.* 2011.** Extracellular invertase is involved in the regulation of clubroot disease in *Arabidopsis thaliana*. *Molecular Plant Pathology* **12**: 247–262.

**Song J, Jiang L, Jameson PE. 2012.** Co-ordinate regulation of cytokinin gene family members during flag leaf and reproductive development in wheat. *BMC Plant Biology* **12**: 78.

**Spichal L. 2012.** Cytokinins – recent news and views of evolutionally old molecules. *Functional Plant Biology* **39**: 267–284.

**Stange RR Jr, Jeffares D, Young C, Scott DB, Eason JR, Jameson PE. 1996.** PCR amplification of the *fas-1* gene for the detection of virulent strains of *Rhodococcus fascians*. *Plant Pathology* **45**: 407–417.

**Stes E, Vandeputte OM, El Jazziri M, Holsters M, Vereecke D. 2011.** A successful bacterial coup d'état: how *Rhodococcus fascians* redirects plant development. *Annual Review of Phytopathology* **49**: 69–86.

**Streubel J, Pesce C, Hutin M, Koebnik R, Boch J, Szurek B. 2013.** Five phylogenetically close rice *SWEET* genes confer TAL effector-mediated susceptibility to *Xanthomonas oryzae* pv. *oryzae*. *New Phytologist* **200**: 808–819.

**Svačinová J, Novák O, Plačková L, *et al.* 2012.** A new approach for cytokinin isolation from Arabidopsis tissues using miniaturized purification: pipette tip solid-phase extraction. *Plant Methods* **8**: 17.

**Tamura K, Dudley J, Nei Ma, Kumar S. 2007.** MEGA4: Molecular Evolutionary Genetics Analysis (MEGA) software version 4.0. *Molecular Biology and Evolution* **24**: 1596–1599.

**Tegeder M. 2012.** Transporters for amino acids in plant cells: some functions and many unknowns. *Current Opinion in Plant Biology* **15**: 315–21.

**Tegeder M, Ward JM. 2012.** Molecular evolution of plant *AAP* and *LHT* amino acid transporters. *Frontiers in Plant Science* **3**: 21.

**Thompson JD, Gibson TJ, Plewniak F, Jeanmougin F, Higgins DG. 1997.** The CLUSTALX windows interface: flexible strategies for multiple sequence alignment aided by quality tools. *Nucleic Acids Research* **25**: 4876–4882.

**Vandesompele J, De Preter K, Pattyn F, *et al.* 2002.** Accurate normalization of real-time quantitative RT–PCR data by geometric averaging of multiple internal control genes. *Genome Biology* **3**: research0034.1–research0034.1.

**Weitbrecht K, Muller K, Leubner-Metzger G. 2011.** First off the mark: early seed germination. *Journal of Experimental Botany* **62**: 3289–3309.

**Wellburn AR. 1994.** The spectral determination of chlorophylls a and b, as well as total carotenoids, using various solvents with spectrophotometers of different resolution. *Journal of Plant Physiology* **144**: 307–313.

**Werner T, Schmülling T. 2009.** Cytokinin action in plant development. *Current Opinion in Plant Biology* **12**: 527–538.

**Zhou J, Peng Z, Long J, *et al.* 2015.** Gene targeting by the TAL effector PthXo2 reveals cryptic resistance gene for bacterial blight of rice. *The Plant Journal* **82**: 632–43.